

Origin of Mining-Induced Fractures Through Macroscale Distortion

White, B. G., Larson, M., and Iverson, S.R.

National Institute for Occupational Safety and Health, Spokane Research Laboratory, Spokane, WA

ABSTRACT: NIOSH researchers have identified a pattern of fracture zone development that suggests an explanation for fracture formation around rectangular openings in underground mines. This pattern is characterized by shearing and dilation that result in either faults or in the repeated formation and propagation of en echelon fractures from sites of tension. Two computer modeling codes, Fast Lagrangian Analysis of Continua (FLAC) and Particle Flow Code (PFC), were used to model different aspects of this pattern. Use of very small elements with FLAC enabled the identification of sites of initial tension near the skin of square-cornered rectangular openings, while PFC allowed the initiation and progressive development of fractures from these sites to be followed as the fractures evolved.

Such studies can lead to a greater understanding of how roof support can be better selected and installed for specific conditions in underground mines prone to roof falls and rock bursts. These studies may also lead to modifications of corner and opening shapes that could be incorporated into mine designs to produce more stable mine openings and reduce the risks of rock falls and rock bursts.

1. INTRODUCTION

Mining-induced fractures are typically either hidden from view or become obscured when fractured rock around mine openings collapses or is ejected in a rock burst. Consequently, knowledge of the distribution, geometry, and extent of mining-induced fractures has been limited. However, fracture patterns that suggest mechanisms of fracture formation are occasionally seen where new crosscuts intersect old ones. The old fractures are exposed in the walls of the new opening, but well-described examples are rare in the literature.

Most investigators agree that extension fractures form parallel to the direction of maximum principal stress. Recently favored explanations for how decimeter and longer (macroscale) fractures develop have mainly involved the proliferation, interaction, and coalescence of smaller fractures.

Fairhurst and Cook [1] proposed that stress-induced microcracks first form an incipient cleavage parallel to the surface of a mine opening. These microcracks then grow into larger fractures as a result of the

applied stress. These fractures shorten with depth, and their ends define a shape concave toward the opening that represents the limit of breakage in the case of a rock burst, roof collapse, or pillar hour-glassing. However, in a field example where thin layers were displayed at the margin of a rock burst breakout, White [2] concluded that the closely spaced fractures had *not* extended across the entire volume of the ejected rock, but were present only near the periphery of the breakout. Other examples that support this scenario are described in White et al.[3]

Stacey [4] proposed that failure about mine openings will occur if extension strain reached a certain value, which he considered a material property. He noted that extension strain is highest near the corners of rectangular openings and suggested that failure begins at these locations. He proposed that the extent of failure is determined by how much rock around the opening exceeds the requisite extension strain. For rectangular openings, critical extension strain is deepest at the midpoint between corners and its limit duplicates the concave shape identified by Fairhurst and Cook [1] and commonly seen after roof falls and

rock bursts. However, Stacey did not differentiate extension resulting from tension from Poisson-response extension. He thought that extension strain causes fracturing even where all normal stresses are compressive, but he did not identify a consistent fracture pattern or a specific mechanism that would cause fracturing to take place.

Diederichs [5] confirmed that tension microfractures form within generally compressive environments and suggested that microfractures may propagate some distance as a result of small, localized, possibly randomly distributed regions of tension. Diederichs considered that interaction of medium-sized fractures leads to large extension fractures. He recognized no specific pattern of large-fracture development about simulated mine openings.

Terrill and VandeKraats [6] reported on an unusual opportunity to view continuous cross sections of mining-induced fractures when a halite roof was excavated higher with a roadheader along 275 m of drift (Figure 1). They concluded that (1) fractures first formed near corners, (2) failure either took the form of a fault that angled upward toward the centerline of the drift or, more commonly, a zone of en echelon extension fractures that possessed similar geometry,

(3) both the zone of en echelon fractures and the fault exhibited a component of slip, (4) dilation of individual extension fractures was pronounced, and (5) the faults and/or fracture zones extended upward from either or both sides of the roof. The observation that the faults and the en echelon fracture zones displayed similar geometries and displacements and also alternated with each other in their development suggests that both types of structures are closely related, which is an idea also considered by Peng and Johnson [7]. Although they documented the essential characteristics of the fractures, Terrill and VandeKraats proposed no specific explanation for them or their consistent patterns.

Based on field and laboratory examples and on Terrill and VandeKraats' descriptions [6], White et al. [3] concluded that a fundamental pattern of fracturing around the periphery of rectangular mine openings involves dilatatory shear zones that originate adjacent to corners and propagate obliquely away from the corners and immediate surface toward the centerline of the drift, as seen in Figure 1. This paper describes continuum and discontinuum models that appear to provide a mechanical explanation for this consistently observed fracture pattern and for creation of the fractures themselves.



Figure 1.—Representative cross section showing fracture patterns in halite roof. (Modified from [6]: Figure 6.)

2. CONTINUUM MODELING

Published continuum models of rectangular mine openings have generally provided no obvious explanation for mining-induced fracture zones about mine openings. However, recognizing that actual fractures are commonly spaced on a scale much narrower than the thickness of the modeling elements typically used, a series of models was constructed using progressive-

ly narrower elements. The goal was to find an explanation for fractures that was not evident in models with larger elements. Although various continuum models are available, the Fast Lagrangian Analysis of Continua (FLAC) [8] computer program was used because of the authors' familiarity with it. A cross section for a square-cornered rectangular drift was initially modeled.

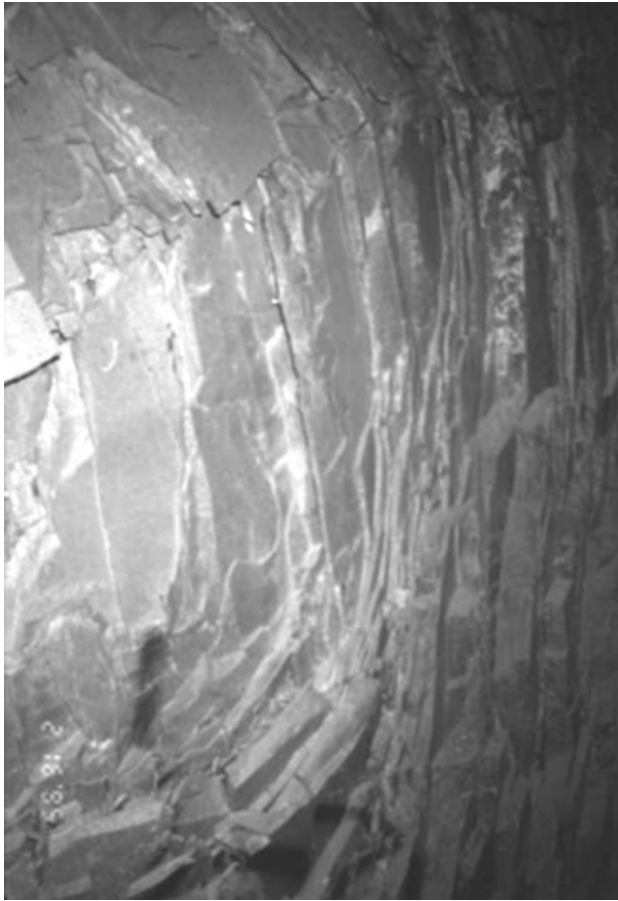


Figure 2.—Narrowly spaced mining-induced fractures at the periphery of a rock burst cavity at a mine in the Coeur d'Alene Mining District. Fractures are spaced 0.5 to 3 cm apart.

In a model with physical properties, stresses, and opening dimensions approximating those in the Coeur d'Alene Mining District (properties of quartzite; 70 MPa horizontal; 35 MPa vertical; 4- by 4.5-m rectangular opening) and model elements similar in thickness to the fracture spacings seen at a Coeur d'Alene rock burst site (0.5 to several centimeters) (Figure 2), sites of high tension were identified near the skin of the opening at short distances from the corners (Figure 3A). In this model, the calculated tension exceeded 24 MPa, more than enough to create a fracture by tension alone using the material properties and stresses assumed. Tension was directed normal to the surfaces so as to produce a fracture parallel to the surface such as was considered by Fairhurst and Cook [1] and commonly viewed in mines. Low-magnitude tension normal to the surface was also distributed toward the centerline of the opening and close to its edge.

From companion results obtained using the Particle Flow Code (PFC) computer program [9], it was

evident that formation of a fracture adjacent to an opening relieves compressive stress in the slab of rock created. Therefore, a fracture was simulated by removing a row of elements containing the initial tension site.

Removal of the immediate element containing the site of high tension in Figure 3A created an elongate region of tension extending diagonally upward and away from the corner (Figure 3B). Within this tensile region, two sites of concentrated tension were evident. The second site was farther upward and beyond the end of the fracture and possessed a lower level of tension.

The effects of propagation of the fracture were then simulated by removing additional elements in the row (Figure 3). As the fracture was extended, the new tension sites described above migrated with the end of the fracture after first separating from and revealing a third tension site. The third site was located deeper in the rock and away from the corner end of the fracture by a distance equal to that of the original tension site from the corner (Figure 3C, 3D). Thus, this tension site duplicated the one associated with the corner, although at a lower level of tension. Yet another site of tension appeared more distant and over this corner (Figure 3D).

Tension at the site at the end of the simulated fracture diminished in magnitude with further extension of the fracture, which would have tended to cause the fracture to stop propagating. In contrast, the amount of tension beyond and above the end of the simulated fracture decreased more slowly as fracture length increased and ultimately exceeded tension at the end of the fracture. This could have promoted formation of a new fracture in an en echelon position with respect to the previous fracture. A factor that was not considered was the influence of maximum principal (compressive) stress on failure, which would also favor fracture initiation at the en echelon position. Finally, tension at all secondary sites was less than tension at the original site, suggesting that formation of new fractures might ultimately cease.

In addition to the work described above, Whyatt [10] confirmed FLAC results with a double-precision modeling run and also duplicated them with the Universal Distinct-Element Code (UDEC) computer program by using model elements similar in size to those used in this study.

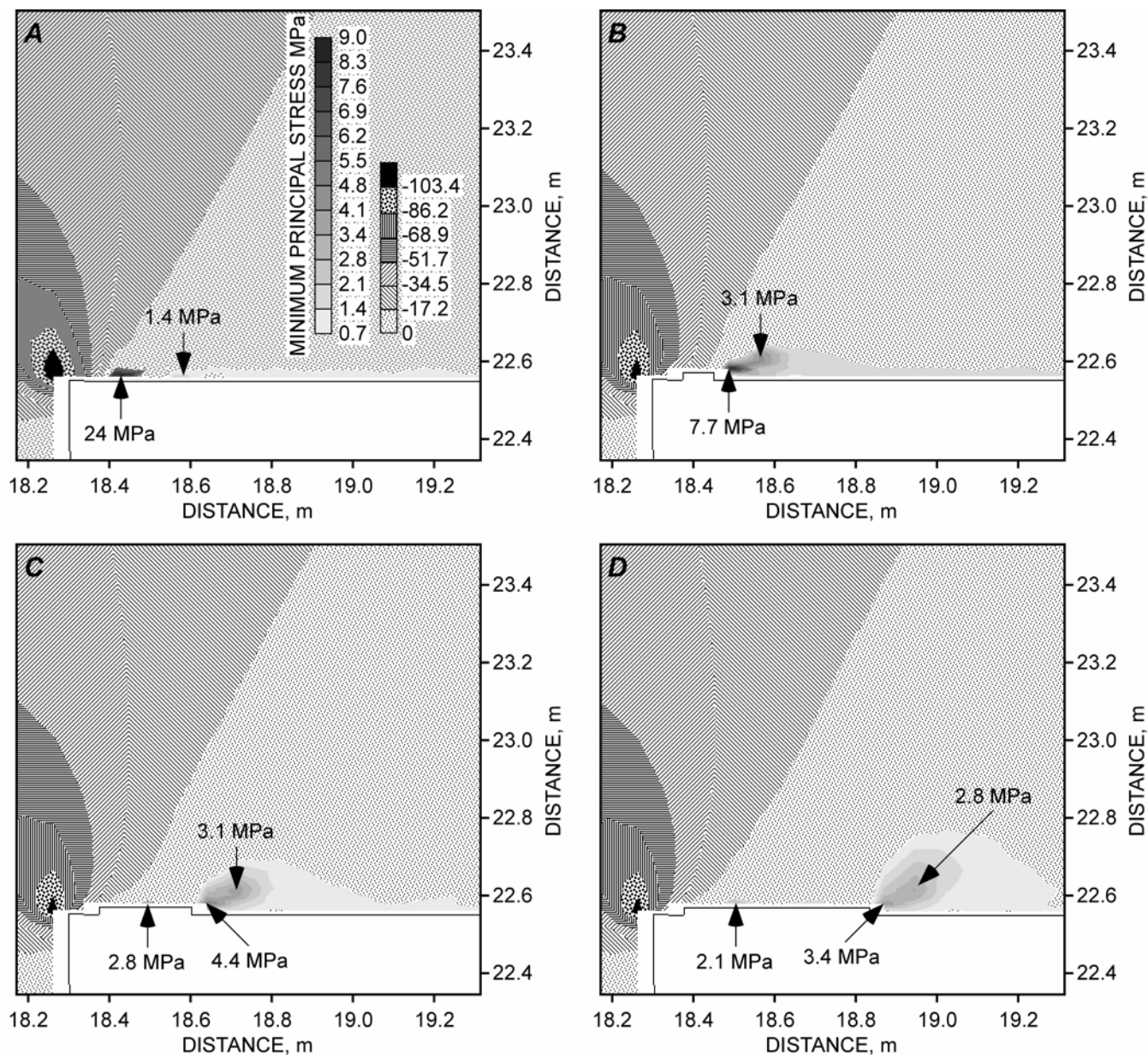


Figure 3.—Portion of FLAC model showing least principal stress near the corner of a rectangular opening for stress conditions and rock properties approximating those of the Coeur d’Alene mining district. Untextured pattern along edge of opening reflects tension. A. Initial model. Tension reached 24 MPa near the corner, but a maximum of only 1.4 MPa along the edge of the roof farther from the corner. B, C, D. Least principal stress for simulated fracture created by removing a progressively longer row of narrow elements, starting (3B) with removal of the element containing the highest stress in A). A region of tension extends diagonally upward to a second site of concentrated tension. C, D. Third and fourth tension sites are revealed as the simulated fracture is extended to right, tensile regime expands, and tension sites at the end of the simulated fracture move with progressive extension of the fracture.

However, although these continuum models identified plausible reasons for (1) initial fracture formation and ultimate stabilization and (2) formation of a new en echelon fracture, the mechanisms responsible for the localized areas of tension that led to this behavior were not obvious. To identify the source of the tension, a discontinuum model using PFC was employed.

3. DISCONTINUUM MODELING

PFC models materials as assemblages of elastic particles bonded together by breakable elastic bonds. Just as with continuum methods, models may be constructed that simulate conditions about mine openings. However, PFC permits failure to take place. Bond stress, displacement from the prior modeling step, and failure show a progression that

can illustrate how mining-induced fractures and fracture zones develop.

A PFC2D simulation was used to investigate the failure process adjacent to a mine opening. Numerous model runs were undertaken using large rectangular blocks of particles containing rectangular openings. Results resembling deformation observed in the field were obtained. However, for the immediate exercise, a model was developed to simulate conditions at a single corner. This made it possible to use smaller particles compared to the scale of the opening while also shortening the run time.

In the simulation, an assemblage of particles was first constructed in the form of a rectangular shape or block. The particles were tightly packed and bonded to simulate a strong homogeneous rock. The assemblage was confined by four walls, which provided a confining pressure of 1.0 MPa. A rectangular portion of the assemblage was then deleted so that the remaining particles formed a notch representing the corner of a mine opening (Figure 4). Opposing walls were then moved inward on one axis at 0.2 m/sec, and the walls in the second axis were controlled to maintain a confining pressure of 1.0 MPa. The inward-moving walls induced a deviator stress onto the assemblage. The walls continued moving inward as the assemblage progressively failed.

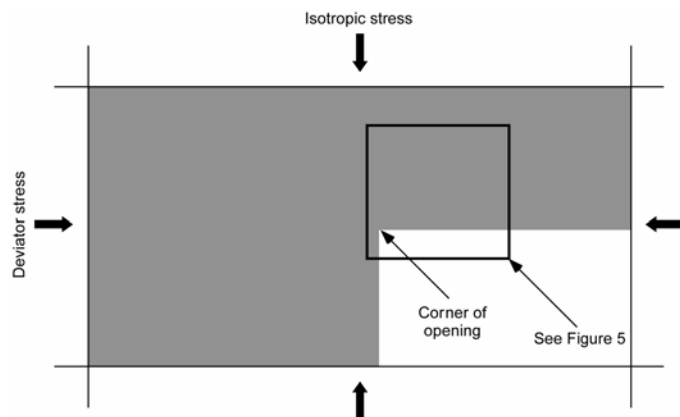


Figure 4.—PFC model formed by loading margins of a rectangular block and then excavating a rectangular area to simulate a cross section of a corner of a mine opening. Horizontal load was then gradually increased so progressive failure could be observed.

The boundary conditions applied to the model are considered to represent only a rough approximation of conditions about mine openings. However, the boundary conditions used for the model resemble those of many reported laboratory strength tests for which Fairhurst and Cook [1] suggested that the resulting fracture patterns simulate those seen in the field. The failure patterns obtained with the PFC model strongly resemble those seen in the laboratory samples as well as in the field, suggesting that the boundary conditions used are reasonable.

Results from the PFC model documented initiation of failure near the corner and propagation of a failure zone away from it and deeper into the model toward the centerline of the simulated opening. Dilation and shear, as seen in the field and reported by Terrill and VandeKraats [6], were also conspicuous.

Although the individual bond failures involved in the creation of the fracture zone included shear failures, tensile bond failures dominated. For the square-cornered model in Figure 4, a long, single fracture parallel to the edge of the opening did not form initially. Instead, an inclined broken zone that manifested comminution, dilatence, and shearing began to develop (Figure 5A). Furthermore, the initial cluster of bond failures did not take place close to the edge of the opening, but at a position where an en echelon fracture might have been expected to form (site X in Figure 5A). As noted in the discussion of FLAC results, only minimal deformation near the edge of the opening was apparently required to cause the tension site that formed in the offset, en echelon position. Therefore, the initial clustering of bond failures at that location may have been promoted by localized elastic deformation at the edge of the opening. This suggests, in turn, that the process zone associated with fault formation is somewhat self-propagating. Laboratory results by Lockner [11] support this interpretation.

Next, bond failures spread downward and approximately half way to the edge of the opening from the initial concentration of bond failures. Additional failures then began near the edge of the opening (Figure 5A, labeled Y) and spread upward until the narrow zone began to fail completely, forming a discrete fault.

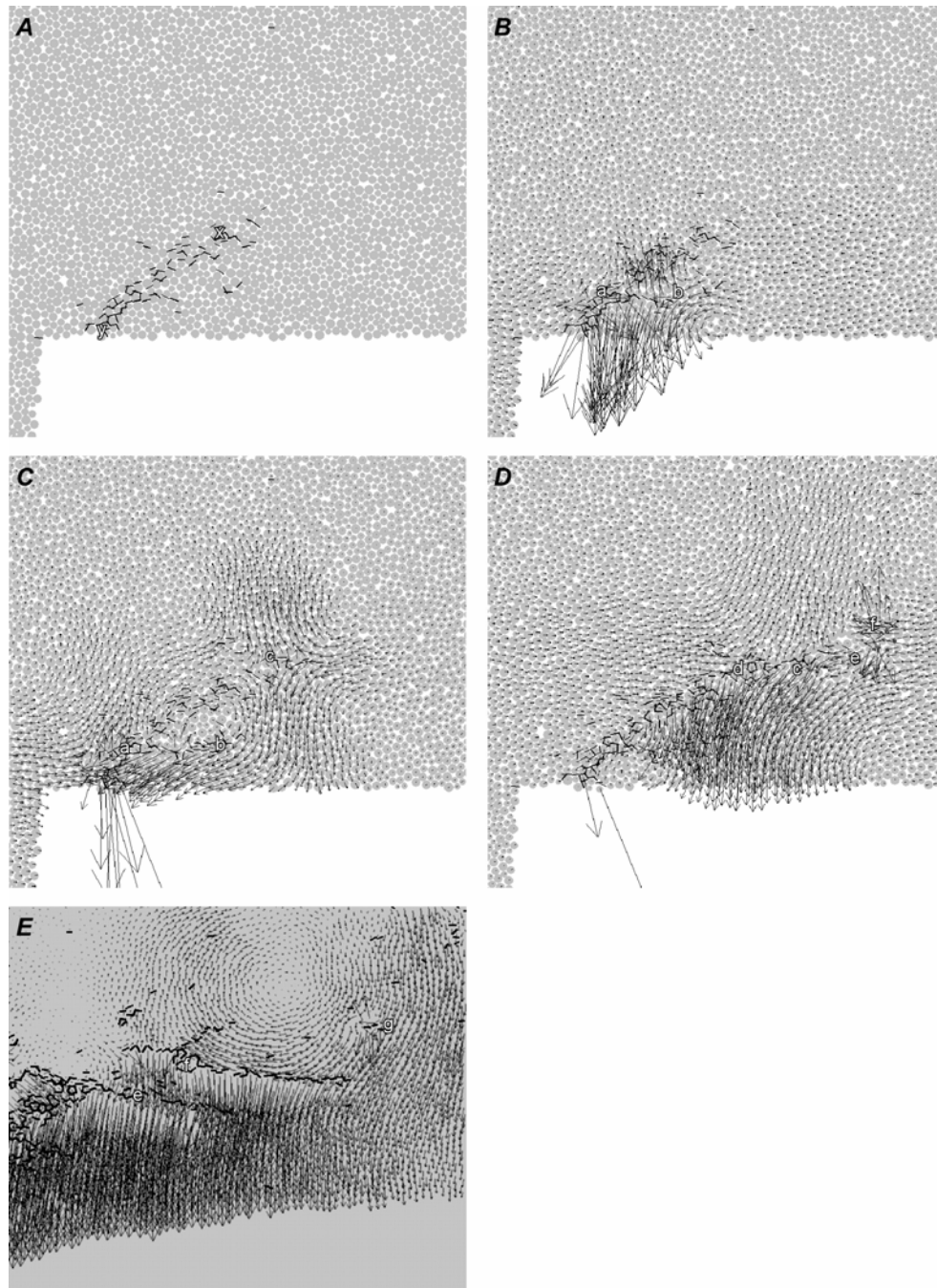


Figure 5.—Stages of progressive failure of square-cornered model. *A.* Early stage of bond failure, identified as short lines. The first clustered failures occurred at site X and spread downward; subsequent failures began and spread upward from site Y. Complete detachment along the lower part of the zone ultimately formed a fault. *B.* Velocity vectors (displacement from previous modeling step) during formation of wing crack a-b. Vectors indicate shear and dilational components along fault portion and also along wing crack. *C.* Velocity vectors as wing crack a-b reached its fullest extent. A new cluster of failures (site of diverging vectors in offset position c) defines early stage of first en echelon fracture. Note scattered distribution of these early failures at this site. *D, E.* Velocity vectors indicating new en echelon fracture d-c-e and sites of initiation of two subsequent en echelon fractures f and g. In *D*, fault zone has propagated to fracture d-c-e and activated it as a wing crack. Each long extension fracture propagated through a series of individual bond failures at fracture tips. Particles not shown in *E*.

When finally a horizontally propagating extension fracture materialized, it began only when the fault was fully detached and had begun to slip (Figure 5*B*). This extension fracture formed at the temporarily stabilized end of the fault. Hence, the fracture was equivalent to

a wing crack forming at the end of a sliding crack, two structures that are normally studied in the form of microcracks. At this point, velocity vectors (displacements from the previous modeling step) (Figure 5*B*) indicated that the fault had become a discrete velocity

discontinuity and also that both extension and shearing were taking place along the fault, as well as at the tip of the developing wing crack.

Here it is of interest to note that wing cracks are typically described as tension cracks. In this case, however, the wing crack exhibited pronounced shearing displacement along its entire length. Numerous PFC model runs indicated that a combination of shear, tension, and extension is, in fact, ubiquitous to extension fractures. Fracture propagation halts when shear and tension at fracture tips cease. This indicates that extension fractures are inherently of mixed mode (involving both tension and shear, or modes I and II, respectively, in the usual nomenclature). Thus, extension fractures cannot form parallel to the direction of maximum principal stress, as is generally assumed, but at some low angle to it (since a plane parallel to the maximum principal stress contains no shear stress).

After the wing crack was well developed, a new concentration of tension failures appeared at a site upward and beyond the end of the wing crack in an offset, en echelon position (Figure 5C). Meanwhile, a near-by area containing some earlier-formed bond failures (labeled X) remained essentially inactive, which suggested that failure development was strongly influenced by imposed, local displacements and that pre-existing areas of weakness that were somewhat removed from such sites might not be involved in the immediate deformation. The newly active site initially formed a rather chaotic cluster of failed bonds, but ultimately developed into a discrete fracture that propagated toward the centerline of the opening in a progression of individual bond failures with no conspicuous process zone development. This fracture ultimately spawned a second en echelon fracture (Figure 5D), which, in turn, led to a third (Figure 5E).

Displacement associated with individual bond failures, as well as failures that extended individual extension fractures, involved lateral convergence of particles toward the tips of propagating fractures. Outward divergence from the actual bond failures and central portions of longer extension fractures reflected extension and tension. However, displacement components parallel to extension fractures on opposite sides of fracture tips and along central portions of active fractures were unequal or were opposite in

direction, reflecting the existence of shear in the plane of the fractures.

As the fracture zone developed, PFC revealed continuously evolving displacements associated with shear along the entire fracture zone, which resulted in localized shear and in divergence that caused extension or actual tension. The PFC model identified fracture formation about the square-cornered opening as resulting from a progression of failures and readjustments that produced additional failures that ultimately extended the greater shear zone.

4. DISCUSSION AND CONCLUSIONS

Field observations have identified a fundamental pattern in mining-induced fractures about rectangular openings. This pattern is characterized by shearing and dilation and the formation of en echelon fractures. An opening surrounded by very small elements was modeled using FLAC. The FLAC models identified sites of high tension near the skin and corner of an opening where an extension fracture would be initiated, propagated away from the adjacent corner, and ultimately stopped as tension at the fracture tip diminished. Meanwhile, a new tension site would develop above and beyond the distal fracture tip in a position that could form a new en echelon fracture. This process would then be repeated until displacements were no longer extensive enough to produce new fractures.

Using PFC, the fracture process was simulated and showed that (1) individual microfractures formed as a result of combined shear and tension and (2) macrofractures propagated by the same basic mechanism. A fault generated with PFC spawned a wing crack, and the wing crack, in turn, spawned an en echelon fracture. Several additional en echelon fractures followed as the final development of the youngest extension fracture in the fracture zone coincided with the creation of a new region of tension where a new en echelon fracture formed.

Incidental observations of interest are that individual macrofractures modeled with PFC propagated in their own plane in combined crack-tip tension and crack-length extension and shear. Based on the current example and on other modeling, such mixed-mode behavior is characteristic of extension fractures. In

general, such fractures form at a low angle to the greatest compressive stress, not parallel to it.

PFC modeling demonstrated minimal process-zone development at the leading edge of extension fractures. No significant direct contribution to fracture formation by interaction and coalescence of microfractures (bond failures) was seen, which suggests that this process is not essential for formation and propagation of individual extension macrofractures. However, coalescence of microfailures was fundamental to fault development.

The concurrence of both FLAC and PFC models with field observation indicates that these methods reasonably simulate the mechanisms of formation of common mining-induced fractures. In subsequent FLAC modeling, it was found that the magnitude of tension near the skin of the opening could be greatly reduced, but not eliminated, by changing the shape of the corner. Rounded corners produced little tension. However, PFC models duplicated the types of failures seen with a square corner, indicating that the fundamental failure patterns and mechanisms remained unchanged. These studies suggest that modifications of corner and opening shapes could be incorporated into mine designs to produce more stable mine openings and reduce the risks of rock falls and rock bursts.

5. REFERENCES

1. Fairhurst, C., and N.G.W. Cook. 1966. The phenomenon of rock splitting parallel to the direction of maximum compression in the neighborhood of a surface. In *Proceedings of the First Congress on the International Society of Rock Mechanics* (Lisbon, Portugal, Sept. 25-Oct. 1, 1966). Lisbon: National Laboratory of Civil Engineers, v. 1, pp. 687-692.
2. White, B.G. 2002. Shear mechanism for mining-induced fractures applied to rock mechanics of coal mines. In *Proceedings, 21st International Conference on Ground Control in Mining*, eds. S.S. Peng et al. (Morgantown, WV, Aug. 6-8, 2002). Morgantown: Dept. of Mining Engineering, WV University, pp. 328-334.
3. White, B., S. Iverson, and M. Larson. 2003. Shear origin of tension in excavation-induced fractures. In *Soil and Rock America 2003. 39th U.S. Rock Mechanics Symposium*, eds. P. Culligan et al. (Massachusetts of Technology, Cambridge, MA, June 22-26, 2003). Vol. I, pp. 909-916.
4. Stacey, R.R. 1981. A simple extension strain criterion for fracture of brittle rock. *Int. J. Rock Mech. & Geomech. Abst.* 18(6): 469-474.
5. Diederichs, M.S. 2002. Stress-induced damage accumulation and implications for hard rock engineering. In *NARMS-TAC 2002: Mining and Tunnelling Innovation and Opportunity*, eds. R. Hammah et al. (July 7-10, 2002, Toronto, ON). Toronto: Univ. of Toronto, v. 1, pp. 3-12.
6. Terrill, L.J., and J.D. VandeKraats. 1997. Case study of conditions observed during the removal of a highly fractured roof beam in bedded halite. In *Proceedings of 16th International Conference on Ground Control in Mining*, eds. S.S. Peng, and C.T. Holland (WV University, Morgantown, WV, Aug. 5-7, 1997). Morgantown: Dept. of Mining Engineering, WV University.
7. Peng, S.S., and A.M. Johnson. 1972. Crack growth and faulting in cylindrical specimens of Chelmsford granite. *Inter. J. Rock Mech. & Min. Sci.* 9: 37-86.
8. Itasca Consulting Group, Inc. (Minneapolis, MN). 1993. *Fast Lagrangian Analysis of Continua (FLAC) User's Manual*.
9. Itasca Consulting Group, Inc. (Minneapolis, MN). 1999. *PFC2D (Particle Flow Code in 2 Dimensions), Version 2.10*.
10. Whyatt, J.K. 2002. Unpublished data from FLAC and UDEC models.
11. Lockner, D. 1993. The role of acoustic emission in the study of rock. *Inter. J. Rock Mech. & Min Sci.* 30 (7): 883-899.